Use of the osmotic membrane bioreactor for the management of tannery wastewater using absorption liquid waste as draw solution

M.J. Luján-Facundo[1*], J.A. Mendoza-Roca[1], J.L. Soler-Cabezas[1], A. Bes-Piá[1], M.C. Vincent-Vela[1], L. Pastor-Alcañiz[2].

[1]Instituto de Seguridad Industrial, Radiofísica y Medioambiental, Universitat Politècnica de València, Camino de Vera, s/n, Valencia 46022 (Spain).

[2]Depuración de Aguas del Mediterráneo (DAM). Avenida Benjamín Franklin, 21. 46980 Parque Tecnológico, Paterna, Valencia (Spain).

Keywords: osmotic membrane bioreactor; tannery wastewater; forward osmosis; reverse salt flux.

Abstract

The performance of an osmotic membrane bioreactor (OMBR) for treating tannery wastewater at laboratory scale has been evaluated in this study. The forward osmosis (FO) membrane tested was CTA-NW from HTI. As draw solution, actual waste water from an absorption column for ammonia separation, which consists mainly of ammonium sulphate was used. The study was focused on the salt reverse flux during the OMBR operation, membrane water flux, biomass characteristics and membrane fouling. Regarding membrane water flux change with the time, the measured values diminished from 3.44 to 0.72 LMH due to the membrane fouling and the salt accumulation in the biological reactor. The stable mixed liquor conductivity value at the end of the

experiment was 29.8 $mS \cdot cm^{-1}$. The chemical oxygen demand (COD) removal efficiencies were maintained near 80% until the first 50 days of operation, considering the soluble COD in the reactor instead of the COD in the membrane permeate for the performance calculation. Thence, COD removal efficiencies decreased progressively due to the accumulation of non degradable COD coming from the tannery wastewater. Concerning to the membrane fouling, FESEM/EDX analysis corroborated that organic fouling was predominant on the membrane active layer.

1. Introduction

Tannery wastewaters are characterized by high organic matter and salt concentration. In a tannery, a series of processes is carried out in order to convert an animal skin into finished leather. For it, several processes with very different characteristics produce pollutants like organic matter from skins, sulfide, lime, sodium chloride, dyes, chromium and organic finishing products that have to be eliminated before their discharge (M. V. Galiana-Aleixandre et al., 2013).

Normally, the effluents of the different processes are divided into two groups: alkaline and acidic streams. Alkaline effluents correspond with those generated by the beamhouse operations like soaking, unhairing and deliming (E. Drioli and B. Cortese 1980; Mendoza-Roca et al., 2010). On the other hand, acidic effluents derive from tanning, dyeing and finishing operations. The conventional treatment of the global effluents consists of a sulfide oxidation of the alkaline stream and physic-chemical treatment of the global wastewaters after homogenization of desulfurized alkaline wastewaters and acidic effluents. Physico-chemical treatments reduce suspended solids and COD and eliminate chromium by precipitation (George et al., 2015; M. Fababuj-

Roger et al., 2007). However, the remaining COD and the high conductivity make difficult its discharge without further treatment. In this way, a biological process would be necessary to reduce the organic matter concentration. Among the biological treatments, sequencing batch reactors (SBR) is commonly used for treating industrial wastewater. Nevertheless, the high slow degradable COD concentration and the settling problems due to high and variable salinity are serious problems in the application of SBRs (Balaguer-Arnandis et al., 2017; Dogruel et al., 2008; Iaconi et al., 2002). The high sludge retention time and the settling elimination make that membrane bioreactors (MBRs) can be considered as an alternative for industrial wastewater treatment (Le-clech et al., 2006; Yang et al., 2006), also producing effluents with higher quality than that of the conventional activated sludge processes (Wang et al., 2016). However, MBR process has a high operating and maintenance cost since it needs a frequent membrane cleaning and high energy consumption (Meng et al., 2009; Wang et al., 2014a).

Recently, a new process combining FO membranes with a biological reactor, named osmotic membrane bioreactor (OMBR), has been introduced as an emerging technology for municipal and industrial wastewater treatments (Achilli et al., 2009; Hau-Ming Chang et al., 2019; Moser et al., 2019). A typical OMBR presents a biological reactor, a FO membrane module and a draw solution (DS) container. The DS generates a high osmotic pressure difference (driving force) between the mixed liquor contained in the biological reactor and the DS. Thus, the effluent from the biological reactor permeates through the FO membrane to the DS container (Holloway et al., 2015; Ryan W. Holloway, 2015; Srinivasa Raghavan et al., 2018).

The main advantage of the OMBR is the high rejection capacity of the FO membranes for trace organic compounds (Xie et al., 2012), pathogens (L. A. Hoover et al., 2011) and ions (Hickenbottom et al., 2013), which makes the product water with an excellent properties. In addition, OMBR offers lower fouling, higher water quality and significantly lower energy demand in comparison with a MBR (Tran et al., 2019; Wang et al., 2016). Although membrane fouling is not the main limiting factor, this phenomenon may also occur.

However, it can be stated that salt accumulation in the bioreactor is the biggest limiting factor (Jie et al., 2012); therefore studies dealing with this problem may be of paramount importance for the OMBR implementation at industrial scale. On the one hand, the high retention capacity of the FO membranes leads to the accumulation in the bioreactor of colloidal matter and dissolved solids (even monovalent salts). On the other hand, the phenomenon of reverse salt flux (RSF) in OMBR implies the transport of salts from the DS into the biological reactor through the FO membrane (Shahzad et al., 2019; Wang et al., 2014b). In this way, salinity build-up in the bioreactor affects the physical and biochemical properties of the activated sludge, increasing the soluble microbial products (SMP) and extracellular polymeric substances (EPS) concentrations in the bioreactor (Wang et al., 2014a) and reduces the membrane water flux since the osmotic driving force goes down.

The treatment of tannery wastewater by an OMBR has not still been studied. It could be an interesting alternative given the above mentioned characteristics of the tannery effluents. In this way, it can be expected an enhancement of the elimination of the slowly degradable organic matter by maintaining high sludge retention times and by its complete separation by the FO membrane.

In this study, the performance of the OMBR process has been evaluated with regard to membrane water flux, RSF, biomass characteristics and membrane fouling. As feed solution (FS), wastewater with increasing contribution of tannery wastewater was used and as DS the effluent from an absorption column for ammonia separation was tested.

2. Materials and methods

2.1. Feed and draw solutions

The FS consisted of tannery wastewater and synthetic wastewater mixed in different proportions according to the planned strategy described in Section 2.3. Actual industrial wastewater from a tannery industry was used as FS. To characterize the four samples tested in this experiment, pH and conductivity measurements were carried out with pH-Meter GLP 21^+ and EC-Meter GLP 31^+ (Crison, Spain), respectively. In addition, the samples of treated effluent were filtered using a 0.45 μm filter reference 16555 from Sartorius (Spain) and soluble fractions were analyzed. In this way, COD, chloride (Cl^-), calcium (Ca^{+2}), NH_4—N, potassium (K^+), magnesium (Mg^{+2}), total nitrogen (TN), nitrates (NO_3-N), nitrites (NO_2-N) and total phosphorous (TP) were determined in the soluble fraction using kits from Merck (Spain). The characteristics of the different samples employed are shown in Table 1.

As simulated wastewater a mixture of bacteriological peptone and meat extract (both supplied by Panreac, Spain) was employed. These chemicals were prepared in order to achieve the same COD concentration that the treated tannery wastewater. In addition, tri-sodium phosphate 12-hydrate (from Panreac, Spain) was used to adjust the phosphorous concentration to ensure the appropriate nutrients amount (COD:N:P relation of 100:5:1 mg·L^{-1}) since the tannery wastewater had very low phosphorous concentration (as it is shown in Table 1).

As draw solution a liquid effluent from an absorption process for ammonia removal was used. The main components were SO_4^{-2} and NH_4-N with concentrations of 153 g·L^{-1} and 19 g·L^{-1}, respectively. The pH and conductivity values of this industrial wastewater were 1.2 and 130 mS·cm^{-1}, respectively. However, pH was adjusted to 4.0 to ensure that the FO membrane was not damaged due to the characteristics of the FO membrane given by the supplier.

Table 1: Characteristics of the wastewater from tannery industry employed as feed solution.

Parameter	Value
pH	8.04-9.29
Conductivity (mS·cm^{-1})	10.8-19.41
COD (mg·L^{-1})	1,497-3,468
SO_4^{2-} (mg·L^{-1})	1,620-3,150
Cl^- (mg·L^{-1})	1,950-4,950
Ca^{2+} (mg·L^{-1})	234-462
NH_4—N (mg·L^{-1})	127-366
K^+ (mg·L^{-1})	8-18
Mg^{2+} (mg·L^{-1})	201-263
TN (mg·L^{-1})	180-530
NO_3-N (mg·L^{-1})	1.6-8
NO_2-N (mg·L^{-1})	0.037-0.848
TP (mg·L^{-1})	0.6-4.4

2.2. FO membrane and OMBR plant

CTA-NW membrane supplied by Hydration Technology Innovations (HTI, USA) was used for the experiments. This FO membrane is a commercial membrane made of cellulose triacetate (CTA) supported by an embedded polyester screen. According to

Cong et al., (2015), the thickness of the membrane was around 50 µm, the contact angle was between 60-80º (what means that the membrane was hydrophilic) and the surface charge was negative at pH higher than 4.5.

The laboratory OMBR plant was equipped with a FO flat sheet membrane module CF042-FO from Sterlitech (USA) with a capacity for one membrane of an effective area of 42 cm^2. The plant also comprised a biological reactor with an effective volume of 1 L and a draw solutions reservoir. The biological reactor contained a mechanical stirrer (Velp Scientifica, Spain) and an air pump Eheim 100 (Eheim, Spain) to maintain the oxygen concentration in the biological reactor around 2 $mg \cdot L^{-1}$. The draw solution tank was located on a digital balance PKP (Kern instruments, Germany), which was connected to a computer registering every 20 minutes the mass variation from the biological reactor to the draw solution using the software "Kern Balance Connection SCD-4.0".

In addition, the feed and the draw solutions were pumped at a flow rate of 30 $L \cdot h^{-1}$ using two peristaltic pumps (Pumpdrive 5006) supplied by Heidolph (Germany). Feed and draw conductivities evolutions were registered using tow conductivity meters model CDH-DS1 from Omega Engineering (United Kingdom). Fig. 1 shows the scheme of the laboratory plant.

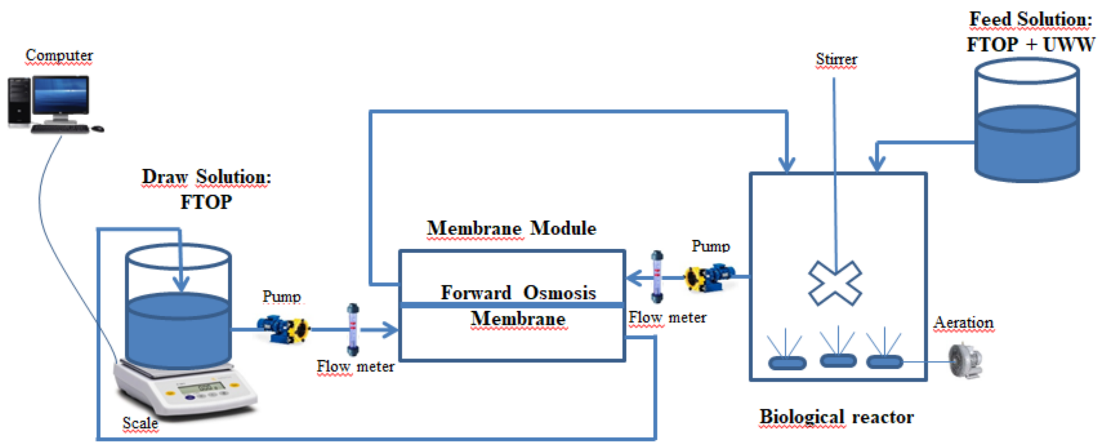

Figure 1: Scheme of the OMBR laboratory plant.

2.3. Experimental procedure

Activated sludge from a municipal wastewater treatment plant (located in Valencia, Spain) was used to inoculate the biological reactor. The total duration of the OMBR experiment was 72 days. The tannery wastewater was mixed with synthetic wastewater increasing the percentage of tannery wastewater progressively in order not to inhibit the biomass.

The mixed liquor suspended solids (MLSS) concentration was maintained at 5 $g \cdot L^{-1}$. The initial pH and conductivity values were 7.4 and 1.30 $mS \cdot cm^{-1}$, respectively. Their variations depended on the permeate flux through the FO. The food to microorganisms (F/M) depended on the characteristics and feed volume of tannery wastewater samples. Anyway, F/M ratio ranged between 0.11-0.33 g $COD \cdot g\ SS^{-1} \cdot d^{-1}$, which corresponded with conventional operating values in activated sludge processes. The reactor was fed once a day, adding a wastewater volume equivalent to the water volume permeated through the FO membrane. After the reactor feeding, an anoxic phase was included to check whether denitrification occurred. The OMBR was operated alternating aerated and non-aerated phases.

Regarding the membrane cleaning procedure, FO membrane was cleaned twice per week. The cleaning step consisted of a backflushing with deionized water as DS and a sodium chloride solution with a concentration of 70 $g \cdot L^{-1}$ as feed solution. In addition, every 28 days, a chemical cleaning step was carried out after the membrane backflushing. For the chemical cleaning step a solution of 1% w/w of Alconox (from Alconox, United States) and 0.8% w/w of EDTA (from Alfa Aeser, United States) were used for the backflushing during 2 hours. After each membrane cleaning step, new fresh DS was prepared for the OMBR operation.

2.4. Analytical methods

2.4.1. Measurement of membrane water flux and reverse salt flux

The pristine FO membrane was characterized measuring the membrane water flux and the RSF. For it, deionized water was used as FS and different concentrations of NaCl were tested as DS (25, 100 and 200 $mg \cdot L^{-1}$). The membrane water flux (J_w, LMH) was determined following Eq.1:

$$J_w = \frac{\Delta V}{A \cdot \Delta t} \quad (1)$$

Where, ΔV is the total volume increase in the draw solution tank (L) measured from the mass variation in a Δt (h) period, and A is the active FO membrane area (m^2). The reverse salt flux Js ($g \cdot m^{-2} \cdot h^{-1}$) was determined following Eq. 2.

$$J_s = \frac{V_t \cdot C_t - V_{t-1} \cdot C_{t-1}}{A \cdot \Delta t} \quad (2)$$

Where, V_t and C_t are the volume and the concentration of sodium chloride in the feed solution measured at time t, respectively.

2.4.2. Water quality parameters

Water quality parameters were measured in the soluble fraction of the biological reactors to check the quality of the treated water. In this way, COD, TN, TP, NH_4^+-N, NO_3-N, NO_2-N, SO_4^{-2}, Cl^-, Ca^{+2} and Mg^{+2} were analyzed (minimum) two times per week. Samples were collected from the bioreactor, were centrifuged at 10,000 rpm for 15 minutes and the supernatant was filtered using a 0.45 μm filter reference 16555 from Sartorius (Spain). All the parameters were determined using kits from Merck.

2.4.3. Mixed liquor characterization

On one hand, mixed liquor suspended solids (MLSS) and mixed liquor volatile suspended solids (MLVSS) concentrations in the bioreactor were measured three times per week following the procedure detailed in ("APHA, AWWA, WEF, Standard Methods for the Examination of Water and Wastewater.," (2005). pH was measured every day with the pH-meter described in Section 2.1.

On the other hand, extracellular polymeric substances in the mixed liquor were extracted using a cation exchanger resin (Dowex Marathon C, Sigma Aldrich, Spain) following the procedure detailed by Zuriaga-Agustí et al., (2013). Extracted EPS (eEPS) and soluble microbial products (SMP) in the reactor were quantified by measuring proteins and carbohydrates concentrations. Protein concentrations were measured using

Bicinchoninic acid (BCA) assay test from Novagen. Carbohydrates were determined applying the Antrone method (Frolund et al., 1996).

2.5. Membrane characterization

2.5.1. Contact angle

The contact angles of the CTA-NW membranes (virgin and fouled) were measured on Dataphysics OCA instrument (Data Physics Instruments GmbH, Filderstadt, Germany). The membranes were cut in pieces of about 60 mm of length and 25 mm of width to carry out the contact angle measurements. The average contact angle (right and left) of 10 extra pure water drops on the membrane surface (10 different locations) was calculated for each membrane.

2.5.2. Field Emission Scanning Electron Microscope

FO fouled membrane surface morphology was examined for damage control and fouling examination with a Field Emission Scanning Electron Microscope (FESEM) Ultra 55 (Zeiss, Oxford instruments, United Kingdom). In conjunction with FESEM, the elemental composition of inorganic deposits attached to the membrane surface was characterized by energy diffusive X-ray (EDX) analyzer with the same microscopy. Before the microscope analysis, fouled membrane was air-dried in a desiccator before being covered with graphite.

3. Results

3.1. Characterization of the virgin membrane

CTA-NW virgin membrane was characterized measuring the water flux and RSF before being used to ensure that there were no membrane defects. These parameters were measured at three different NaCl concentrations in the DS and using deionized water as FS. In addition, the average contact angle and zeta potential are summarized in Table 2. Regarding J_w and J_s, relatively similar values were reported in the literature. For example, Yang et al., (2016) published a J_w of 4.79 LMH and Bell et al. (2016) reported a J_s value of 5.5 $g \cdot m^{-2} \cdot h^{-1}$ (both using as DS a NaCl solution with a concentration of 58.4 $g \cdot L^{-1}$). According to Vatanpour et al., (2014), there are three important parameters that control the membrane fouling: hydrophilicity (associated from contact angle), surface charge and surface roughness. As previously published Muthu et al., (2014), it is considered membranes are hydrophilic if the contact angle is lower than 90º. In this way, the contact angle measured for the CTA-NW membrane was 54.0º indicates that the membrane is moderately hydrophilic. This result is very similar to the study published by (Luo et al., 2017b), who reported a contact angle value of 60.4º. The zeta potential value was reported by (Bell et al., 2016) and was -10 mV at pH4, these group of authors also published that membrane becomes more negatively charged by the pH.

Table 2: CTA NW virgin membrane properties.

NaCl ($g \cdot L^{-1}$)	**Water flux (LMH)**	**RSF ($g \cdot m^{-1}$ h^{-1})**	**Contact Angle (º)**	**Zeta potential at pH 4 (mV)[a]**
25	2.15 ± 0.19	1.36 ± 0.65		
100	4.49 ± 0.18	2.89 ± 0.57	54.0 ± 2.8	-10.00
200	6.5 ± 0.33	3.2 ± 0.4		

a) Values from previous publication [31].

3.2. Water flux and salinity build-up in the bioreactor

Fig.2.a illustrates the FO membrane water flux evolution during the OMBR operation. Each vertical line represents a cleaning step (clear lines represent a backflushing and the dark lines show a backflushing followed by a chemical cleaning). As observed in Fig. 2.a, membrane water flux decreased during the whole experiment. According to Luo et al., 2017a, the water flux decline could be attributed to a reduction of the effective trans-membrane osmotic pressure (due to salinity build-up in the bioreactor and a decrease of the concentration of the draw solution) and to membrane fouling. Membrane water flux change through the time (Fig. 2.a) shows three different stages; the first one occurs until the 30-th operation day, the second one from the 30-th day to the second chemical cleaning and the third one from the second cleaning onwards. On one hand, during the first stage (days 0-30), the membrane water flux decreased from 3.5 LMH to around 1.5 LMH what could be related to the deposition of foulants on the membrane surface (Zou et al., 2013). Although flux decrease was not very high, irreversible fouling occurred since the backwashing became progressively less effective. During the second stage, the fouling was more severe, decreasing the permeate flux to values lower than 1 LMH. The highest flux decay coincided with the feeding of the reactor with 100% of tannery wastewater. This implies that the non degradable COD of the tannery wastewater played an important role on membrane fouling. Finally, after the second chemical cleaning, the evolution of the permeate flux was very similar to that obtained for the first operating stage. This could be achieved after reducing the percentage of tannery wastewater in the reactor feed (Fig. 2.b). In general terms, several authors like Luo et al., (2016b) and Wang et al., (2017) have reported similar tendencies of the OMBR operating flux.

Fig. 2.b shows the mixed liquor conductivity evolution and the tannery waste water percentage applied during the OMBR experiment in the feed solution. As expected, the

high rejection capacity of the FO membrane associated with the RSF caused salinity build-up in the biological reactor. In this way, as it can be observed in Fig. 2.b, the mixed liquor conductivity increased progressively during the experimental period until reaching a final value around 29.8 $mS \cdot cm^{-1}$. It is important to highlight that an increase of the percentage of tannery wastewater in the composition of the feed solution drove to a conductivity increase in the mixed liquor, due to the salinity of the tannery effluent. In addition, from the day 35-th of operation onwards, less significant mixed liquor conductivity increase was observed due to the concentration polarization phenomena that diminish the effective difference of salts concentration between both membrane sides. It also implies a diminution of the membrane water flux. Finally, daily sampling and several sludge withdrawals (to maintain stable the biomass concentration and control the sludge retention time) were carried out contributing to moderate the mixed liquor conductivity increase. The same tendency, salinity accumulation in the biological reactor, was previously published by others OMBR studies like (Chang et al., 2019; Luo et al., 2017b; Tran et al., 2019).

a)

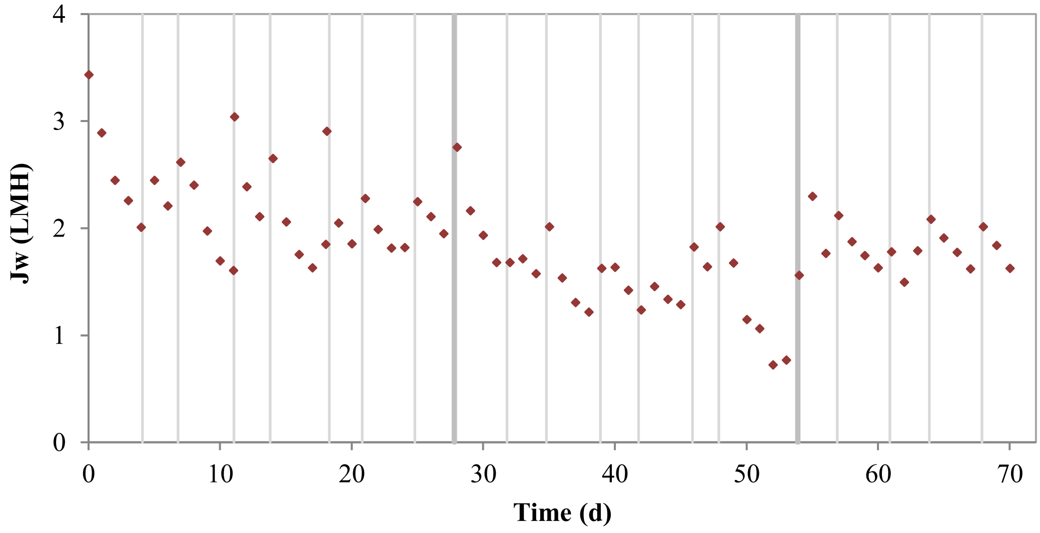

b)

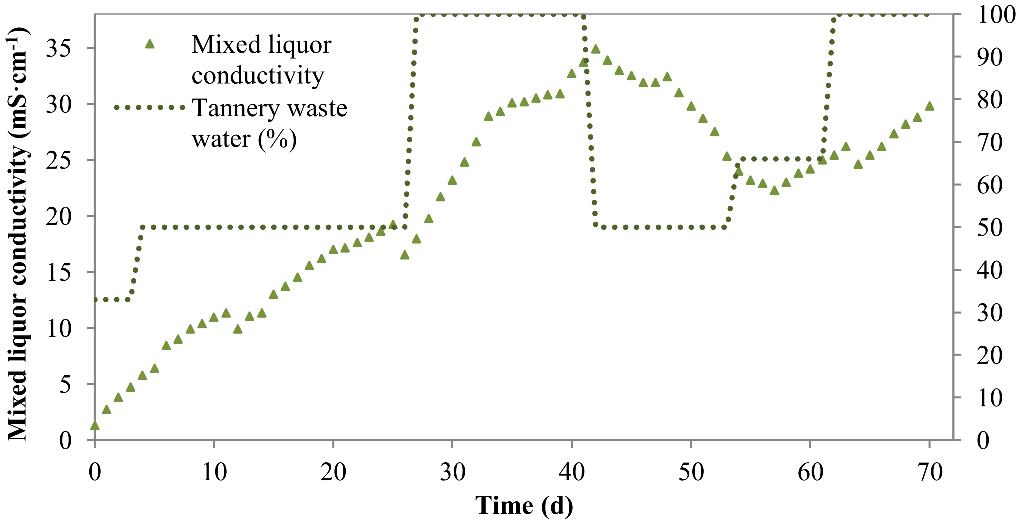

Figure 2: a) Membrane water flux evolution and b) mixed liquor conductivity evolution and tannery waste water percentage applied during the OMBR experiment.

3.3. Organic matter, nitrogen and other ions in the OMBR

Organic matter, nutrients and Ca^{+2}, Mg^{+2}, Cl^{-} and SO_4^{-2} concentrations in the mixed liquor supernatant were analyzed to evaluate the OMBR performance. Fig. 3 shows the biological COD removal efficiencies during the experimental period. However, the FO membrane rejected practically all the organic matter (COD in the DS was negligible). In this way, the total COD removal efficiency was higher than 98% during all the experiment. Thus, COD removal was calculated in this manuscript from the soluble COD content in the biological reactor instead of measuring the COD concentration in the DS, with the aim of reflecting the changes in the biological process performance. As it can be observed in Fig. 3, a decrease of the OMBR performance with the time was observed. This fact could be mainly related with the progressive accumulation of non-degradable organic matter and cellular debris in the biological reactor due to the high FO rejection capacity (almost 100% as previously commented) (Chen et al., 2013; Qiu, G. et al., 2015). In addition, the high salinity content in the bioreactor could significantly affect the microbial metabolism and damage the biological treatment (Lay et al., 2010).

In spite of the slight gradual decrease, the soluble COD removal efficiency was maintained near 80% until the 50^{th} day. Accumulated COD was due to the non-degradable COD, whose value ranges between 400 and 600 $mg \cdot L^{-1}$ according to the bibliography (Balaguer-Arnandis et al., 2017). As the tannery wastewater was fed to the reactor together with synthetic wastewater, the non-biodegradable COD was reduced by the dilution effect and the by the sludge withdrawals. However, after having fed the reactor only with tannery wastewater, the accumulation of refractory COD implied a diminution in the organic matter removal performance and also a flux diminution as commented above. Therefore, it can be concluded that the treatment by OMBR of industrial wastewaters with considerable non-biodegradable COD may lead to operation problems when the sludge withdrawals frequency do not let decreasing the non-biodegradable COD in the reactor.

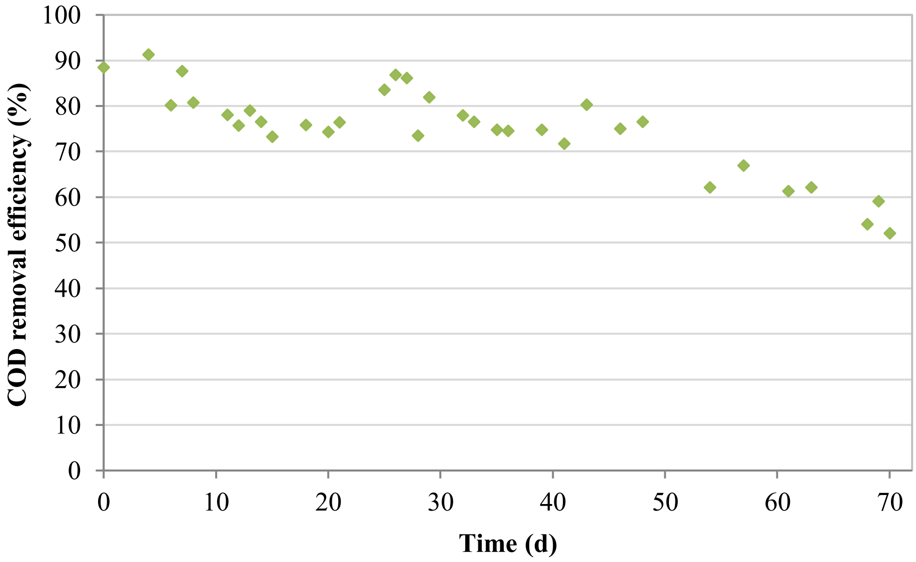

Figure 3: COD removal efficiency during the experimental period.

The reverse ammonium-nitrogen flux from draw solution to the biological reactor makes of special interest the study of the eventual nitrogen removal. Thus, a non-aerated phase was included in the OMBR operation to evaluate whether denitrification was possible. In this way, Fig. 4 shows the evolution of nitrogen concentrations in the mixed liquor supernatant during the experimental period. It was observed a gradual increase of TN and NH_4^+-N during the OMBR operation until reaching a final value of 1,000 and 848 mg·L^{-1}, respectively. The N balance in the reactor has to consider two influents, which are the feed stream and the global RSF (it includes nitrogen that can pass through the membrane since rejection is not 100%), the elimination by biomass assimilation or by assimilation plus biological denitrification and the sludge withdrawal. Table 3 illustrates the expected N-NH_4 concentration if the N-NH_4 balance is carried out. The expected N concentration at the end of each period has been calculated as the sum of four terms. These are the N-NH_4 mass entering the reactor, the N-NH_4 concentration at the beginning of the period, the estimated value for the global RSF and the sludge withdrawn (negative term), considering the period duration and the volume of the reactor (1 L). A global specific N-NH_4 reverse flux of 60 mg·L^{-1} was considered since it was measured in previous FO tests using deionized water as FS and the same ammonia absorption effluent as DS (Soler-Cabezas et al., 2018).

Focusing on the values illustrated in Table 3, it has to be commented that nitrogen removal in the reactor was decreasing with the time. It can be confirmed that biological denitrification occurred until 26th day due to the high removal efficiencies. It has to be highlighted that contradictory results have been found in the literature concerning the nitrogen removal in tannery wastewaters. In this way, some authors reported about nitrification inhibition with this type of wastewaters. As an example, a mean nitrification performance of 18% in a SBR treating tannery wastewater was reported by R. Ganesh et al., 2015. G. Munz et al., 2009 also reported reduced nitrification processes in the biological treatment of tannery wastewaters without finding a particular substance responsible for the ammonium oxidation bacteria inhibition. On the contrary, Carucci et al. (1999) reported a complete nitrification and high nitrogen removal efficiencies treating tannery wastewaters in a sequencing batch reactor.

From 27th day on, the nitrogen removal efficiency in the reactor decreased, ranging between 18 and 34%, which was due to biomass assimilation rather than nitrification-denitrification. In this way, the measured N-NO_2 and N-NO_3 (Fig. 4) did not mean that simultaneous nitrification-denitrification occurred. The inhibition of ammonium oxidizing microorganisms might be caused by the increasing refractory COD and by the increasing ammonia concentration in the OMBR.

Table 3: Estimated N-NH4 biological removal.

Period (d)	Expected mean N-NH4 concentration ($mg \cdot L^{-1}$)	N-NH4 measured concentration ($mg \cdot L^{-1}$)	Estimated N-NH4 biological removal (%)
1-4	183.46	1	99.45
5-26	1,335.82	411	69.23
27-41	852.08	660	22.54
42-53	1,011.00	662	34.52
54-61	923.46	762	17.48
62-70	1,070.48	848	20.78

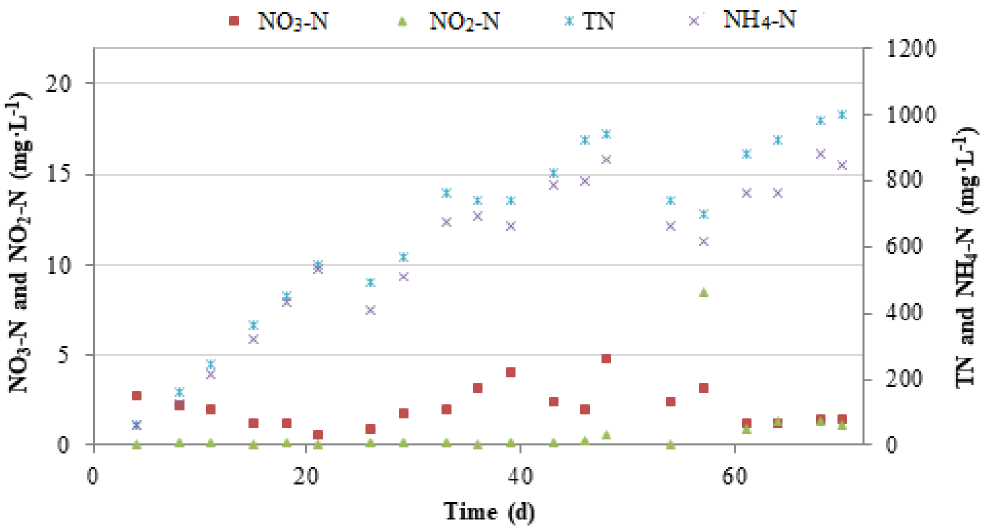

Figure 4: Nutrients evolution in the feed solution during the experimental period.

Fig. 5 represents SO_4^{2-}, Cl^-, Ca^{2+} and Mg^{2+} accumulations in the bioreactor. Focusing on SO_4^{2-}, what is the main component of the DS apart from the ammonium nitrogen, it is important to remark that its high reverse flux due to Fick's law was the cause of the high SO_4^{-2} concentration in the biological reactor (its concentration was multiplied by more than 5 times in the operation time). Cl^-, Ca^{2+} and Mg^{2+} concentrations also increased progressively in the OMBR due to their rejection by the FO membrane. In spite of the high reached concentrations, no salt precipitation was observed in the FESEM/EDX analysis as shown in Section 3.5.2.

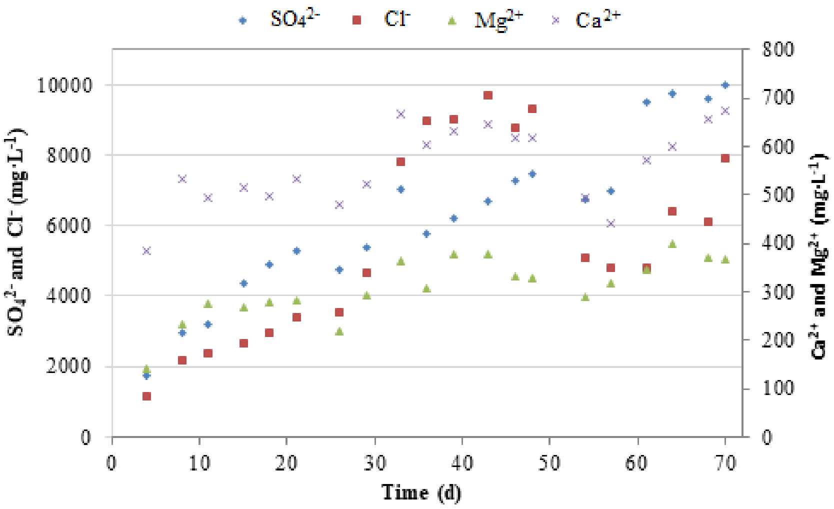

Figure 5: Ions evolution in the feed solution during the experimental period.

3.4. Mixed liquor characteristics

3.4.1. Mixed liquor pH and VSS

Fig. 6 shows pH and VSS percentage evolution during the OMBR operation. As it can be observed, mixed liquor pH increased up to 8.24 within the first 54 days of operation. This fact was caused by the forward diffusion of protons from the mixed liquor into the draw solution and by the reverse transport of cations to maintain the electroneutrality of the mixed liquor (Luo et al., 2016). However, when the water and salt reverse fluxes decreased (from day 50-th onwards, as it can be seen in Fig. 2), no relevant pH increase was observed thereafter. The same trend was published by Luo et al., (2016a), who operated an OMBR with different draw solutes observing a similar evolution.

The percentage of VSS decreased during the OMBR operation from 85.71% to 64.44% (Fig. 6) due to the alteration in the biomass activity caused by salinity build-up in the bioreactor. This observation was in agreement with previous studies (Luo et al., 2016a; Wang et al., 2014b) which reported that salinity increase causes the inhibition on biomass growth and activity.

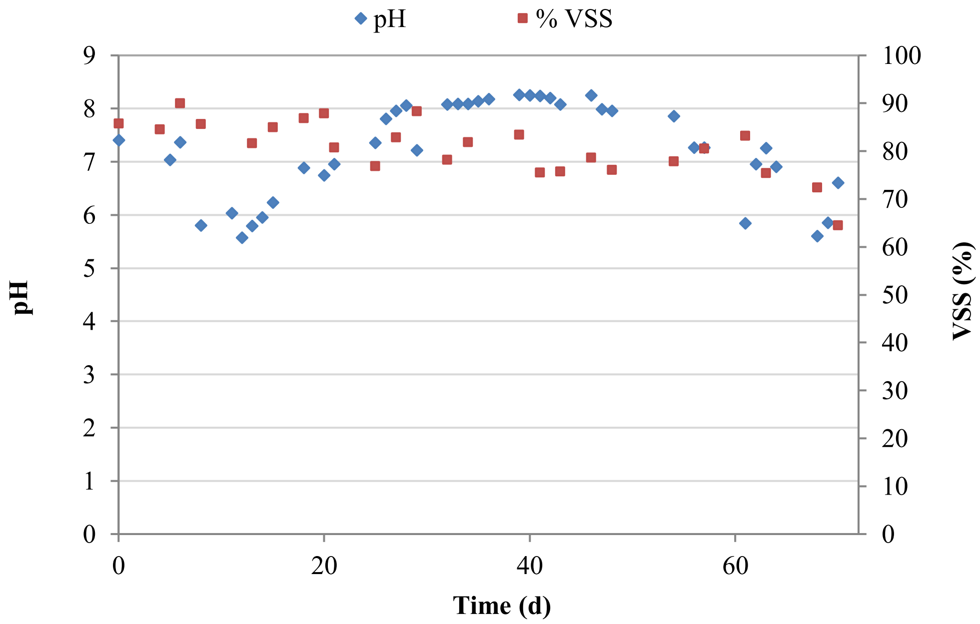

Figure 6: pH and VSS evolution.

3.4.2. EPS analysis

The chemical characterization of the mixed liquor in terms of proteins, carbohydrates and DNA concentrations is important since salinity build-up in the biological may modify their concentrations, affecting both the reactor performance and the membrane fouling. Microbial response to salinity build-up results in a more SMP and eEPS concentrations (Luo et al., 2016a) and (Priscila B. Moser et al., 2019) . Fig. 7.a and Fig. 7.b represents the evolution during the experimental period of SMP and eEPS concentrations in terms of proteins and carbohydrates, respectively. SMP concentrations in terms of proteins increased gradually during the experimental period as mixed liquor conductivity increased. From the day 42-th of operation, SMP concentrations decreased due to the salinity biomass acclimation. SMP concentrations concerning carbohydrates significantly increased until the day 14-th of operation. Thereafter, SMP concentrations became more stable and varied from 17.8 $mg \cdot L^{-1}$ until to 49.08 $mg \cdot L^{-1}$. Zhang et al., 2017 operated an OMBR using NW-CTA FO membrane and published that SMP concentrations increased as mixed liquor salinity increases meanwhile EPS concentration was fairly stable.

On the contrary, there was not influence of the salinity increase on the eEPS concentration, which was almost constant during the operation time. Only for protein concentrations, eEPS slightly increased until reaching a maximum value of 171.45 mg·g VSS^{-1}. The highest values coincided with the samples taken after feeding the reactor only with tannery wastewater, which increased the bacteria stress considerably. At the end of the operation time, eEPS concentration reached values in the same range than the initial ones. An explanation for the constant eEPS values was reported by Luo et al., 2016a, who stated that there were changes in the eEPS concentrations probably because of the equilibrium between their release and hydrolysis.

a)

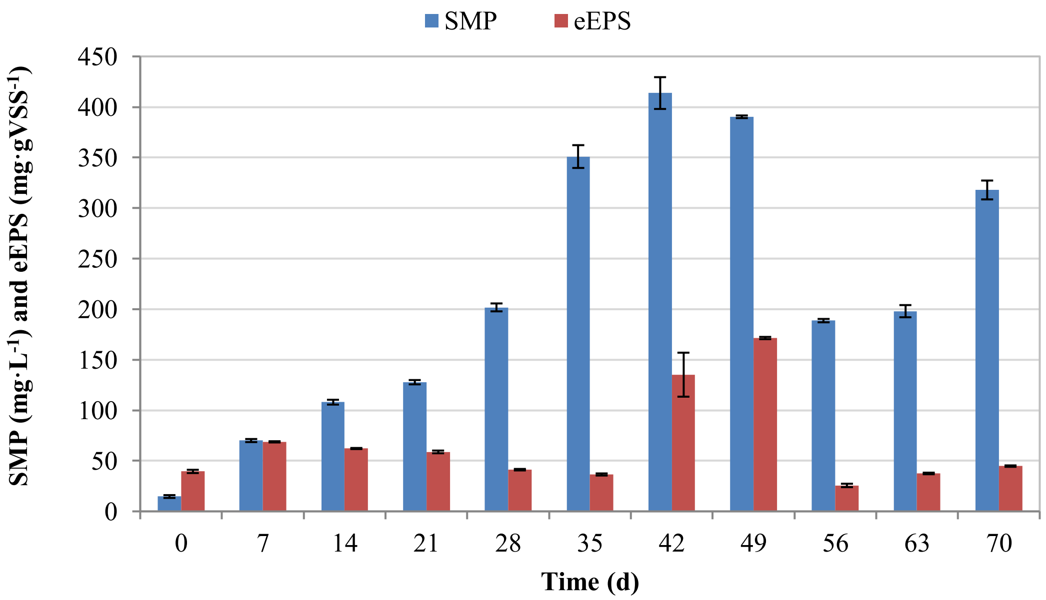

b)

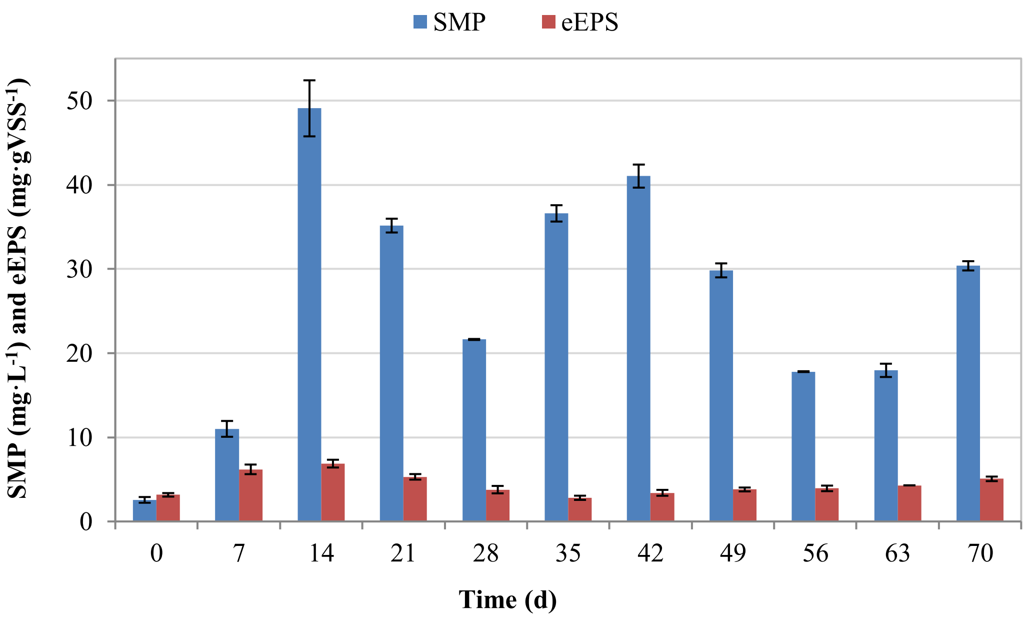

Figure 7: SMP and eEPS concentrations in terms of (a) proteins and (b) carbohydrates.

3.5. Membrane characterization

3.5.1. Contact angle measurement

Contact angle measurement of fouled FO membrane was evaluated to complete the characterization of the membrane surface. Contact angle indicates the degree of hydrophilicity of membrane and it depends on the membrane porosity and membrane material (Susanto and Ulbricht, 2007). The contact angle of the FO fouled membrane was 80.22º ± 6.86º. This value was higher than the contact angle of the pristine membrane showed in Table 2 (54.0º ± 2.8º) what indicates than the presence of microbial residues or foulants on the membrane surface can modify the property of the membrane more hydrophobic (Luo et al., 2016c).

3.5.2. FESEM analysis

Microscopy analysis was performed in the active layer of the fouled FO membrane to study the membrane fouling. Fig. 8 illustrated an image of the membrane surface morphology. As it can be observed in Fig. 8, foulant clusters were detected over the membrane surface. In this way, Zhang et al., 2012 studied the membrane biofouling and scaling in OMBR and concluded that the fouling mainly occurred in the membrane surface instead of in the internal pore. The formation of the cake layer increases the membrane resistance and confirms the membrane flux reduction showed above in Fig. 2.a.

Fig. 9 shows EDX analysis of the fouled FO membrane and Table 4 summarize the average (16 zones of the active layer were evaluated) element weight percentage of foulants on the fouled FO membrane. It can be mainly observed the presence of C and O due to the membrane material (CTA). However, more elements were detected such as Na, Mg, Ca, P, S, Cl although in a very small percentages. This confirms that organic fouling was predominant over the inorganic fouling.

Table 4: Element weight percentage of foulants on fouled FO membrane.

Element	Wt (%)
N	3.65
O	90.09
Na	0.48
Mg	0.55
P	1.01
S	3.57
Cl	0.29
Ca	0.36

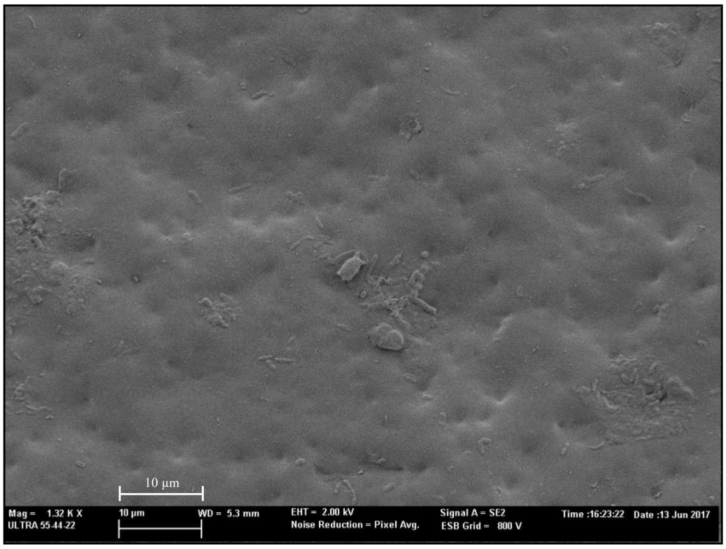

Figure 8: FE-SEM image of active layer of fouled FO membrane.

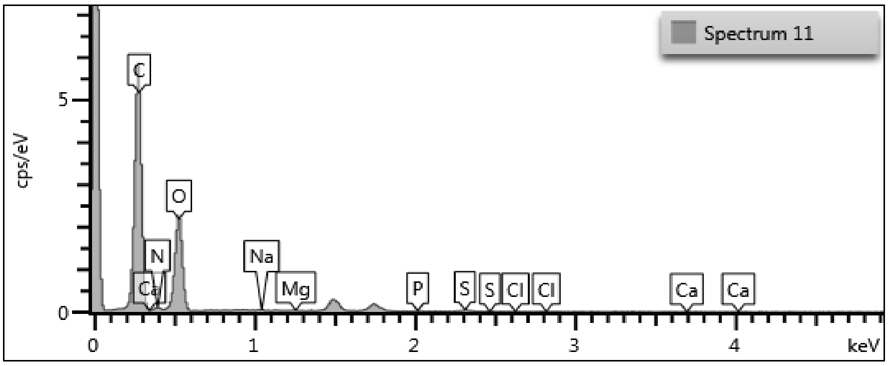

Figure 9: EDX analysis of the FO fouled membrane.

4. Conclusions

An OMBR has been operated for continuous treatment of tannery wastewater. The tannery wastewater fed to the reactor was increased gradually in order to maintain COD removal efficiencies around 80%. Actual wastewater that mainly consisted of ammonium sulphate provided enough driving force in terms of osmotic pressure difference between both sides of the membrane for the operation of the OMBR. Dilution of this stream in the process could facilitate its use in the agriculture.

In this way, it can be concluded that OMBR was efficient for COD removal from tannery wastewaters. In addition, the DS was an actual industrial effluent, saving the costs related to DS regeneration, which are important in forward osmosis processes. Nevertheless, inhibition of nitrification was observed due to increasing COD and ammonia accumulation in the reactor. On the other hand, the progressive salinity build-up in the biological reactor caused several changes in the biomass characteristics and a decrease in the membrane water flux.

The feasibility of the process at a higher scale will be based on controlling the accumulation of the refractory COD of the tannery wastewater and on the further use of the diluted DS.

Acknowledgments

This study was supported by the Spanish Ministry of Economy and Competitiveness through the project RTC-2015-3582-5-AR.

References

Achilli, A., Cath, T.Y., Marchand, E.A., Childress, A.E., 2009. The forward osmosis membrane bioreactor : A low fouling alternative to MBR processes. Desalination 239, 10–21.

APHA, AWWA, WEF, Standard Methods for the Examination of Water and Wastewater., 2005. Washington.

Frolund, B., Palmgren, R., Keiding, K H.N., 1996. Extraction of extracellular polymers from activated sludge using a cation exchange resin. Water Res. 135, 1749–1758.

Balaguer-Arnandis, E., Cuartas-Uribe, B., Bes-Piá, M.A., Mendoza-Roca, J.A., Galiana-Aleixandre, M.V., 2017. Performance Improvement of a Sequencing Batch Reactor for Treating Tannery Wastewaters. Chem. Eng. Technol. 40, 1666-1673.

Bell, E., Holloway, R.W., Cath, T.Y., 2016. Evaluation of forward osmosis membrane performance and fouling during long-term osmotic membrane bioreactor study. J. Memb. Sci. 517, 1–13.

Carucci, A. Chiavola, M. Majone, E. Rolle. Treatment of tannery wastewater in a sequencing batch reactor, 1999. Water Sci. Technol 40 (1), 253-259.

Chen, L., Gu, Y., Cao, C., Zhang, J., Ng, J., 2013. Performance of a submerged anaerobic membrane bioreactor with forward osmosis membrane for low-strength wastewater treatment. Water Res. 50, 114-123.

Cong, N., Chen, S., Thi, H., Hao, H., Guo, W., Wen, C., Lin, P., 2015. Applicability of a novel osmotic membrane bioreactor using a speci fi c draw solution in wastewater treatment. Sci. Total Environ. 519, 586–594.

Dogruel, S., Dulekgurgen, E., Orhon, D., 2008. COD fractionation of tannery wastewaters — Particle size distribution , biodegradability and modeling. Water Res. 42, 1083–1092.

Drioli E., Cortese B., 1980. Ultrafiltration processes for pollution control and chemical reuse in the tanning industry. Desalination 34, 131–139.

Galiana-Aleixandre, M.V., Mendoza-Roca, J.A, Bes-Piá, A., 2013. Reducing the pollution from tanneries by process wastewater reuse and membrane technologies, in: Waste Water Reuse and Management. Chapter from book Wastewater reuse and Management. pp. 105–125.

Ganesh, R., Sousbie, P., Torrijos, M., Bernet, N., Ramanujam, R.A., 2015. Nitrification and denitrification characteristics in a sequencing batch reactor treating tannery wastewater. Clean Technol. Environ. Policy 17, 735–745.

George, J.S., Ramos, A., Shipley, H.J., 2015. Tanning facility wastewater treatment : Analysis of physical – chemical and reverse osmosis methods. J. Environ. Chem. Eng. 3, 969–976.

Hau-Ming Chang, Yung-Chun Sun, I-Chieh Chien, Wen-Shing Chang, Saikat Sinha ray, Dan Thanh Ngoc Cao, Chinh Cong Duong, Shiao-Shing Chen, 2019. Innovative upflow anaerobic sludge osmotic membrane bioreactor for wastewater treatment. Bioresour. Technol. 287. Art 121466.

Hickenbottom, K.L., Hancock, N.T., Hutchings, N.R., Appleton, E.W., Beaudry, E.G., Xu, P., Cath, T.Y., 2013. Forward osmosis treatment of drilling mud and fracturing wastewater from oil and gas operations. Desalination 312, 60–66.

Holloway, R.W., Wait, A.S., Fernandes, A., Herron, J., Schutter, M.D., Lampi, K., Cath, T.Y., 2015. Long-term pilot scale investigation of novel hybrid ultra fi ltration-osmotic membrane bioreactors. Desalination 363, 64–74.

Iaconi, C. Di, Lopez, A., Ramadori, R., Pinto, A.C. Di, Passino, R., 2002. Combined chemical and biological degradation of tannery wastewater by a periodic submerged filter (SBBR). Water Res. 36, 2205–2214.

Mendoza-Roca, J.A., Galiana-Aleixandre, M.V., Lora-García, J., Bes-Pià, A. 2010. Purification of tannery effluents by ultrafiltration in view of permeate reuse. Sep. Purif. Technol. 70, 296–301.

Jie, W., Zhang, J., Lay, W.C.L., Cao, B., Fane, A.G., Liu, Y., 2012. State of the art of osmotic membrane bioreactors for water reclamation. Bioresour. Technol. 122, 217–222.

Laura A. Hoover, William A. Phillip, Alberto Tiraferri, Ngai Yin Yip, and M.E., 2011. Forward with Osmosis: Emerging Applications for Greater Sustainability. Environ. Sci. Technol. 45, 9824–9830.

Lay, W.C.L., Liu, Y., Fane, A.G., 2010. Impacts of salinity on the performance of high retention membrane bioreactors for water reclamation: A review. Water Res. 44, 21–40.

Le-clech, P., Chen, V., Fane, T.A.G., 2006. Fouling in membrane bioreactors used in wastewater treatment. J. Memb. Sci. 284, 17–53.

Luján-Facundo, M.J., Soler-Cabezas, J.L., Mendoza-Roca, J.A., Vincent-Vela, M.C., Bes-Piá, A., 2017. A study of the osmotic membrane bioreactor process using a sodium chloride solution and an industrial effluent as draw solutions. Chem. Eng. J. 322, 603–610.

Luo, W., Hai, F.I., Price, W.E., Elimelech, M., Nghiem, L.D., 2016a. Evaluating ionic organic draw solutes in osmotic membrane bioreactors for water reuse. J. Memb. Sci. 514, 636–645.

Luo, W., Hai, F.I., Price, W.E., Guo, W., Ngo, H.H., Yamamoto, K., Nghiem, L.D., 2016b. Phosphorus and water recovery by a novel osmotic membrane bioreactor – reverse osmosis system. Bioresour. Technol. 200, 297–304.

Luo, W., Phan, H. V, Xie, M., Hai, F.I., Price, W.E., Elimelech, M., Nghiem, L.D., 2017a. Osmotic versus conventional membrane bioreactors integrated with reverse osmosis for water reuse: Biological stability, membrane fouling, and contaminant removal. Water Res. 109, 122–134.

Luo, W., Xie, M., Hai, F.I., Price, W.E., Nghiem, L.D., 2016c. Biodegradation of cellulose triacetate and polyamide forward osmosis membranes in an activated sludge bioreactor : Observations and implications. J. Memb. Sci. 510, 284–292.

Luo, W., Xie, M., Song, X., Guo, W., Ngo, H.H., Zhou, J., Nghiem, L.D., 2017b. Biomimetic aquaporin membranes for osmotic membrane bioreactors: Membrane performance and contaminant removal. Bioresour. Technol. 249, 62–68.

Fababuj-Roger, M., Mendoza-Roca, J.A., Galiana-Aleixandre M.V., Bes-Piá A., Cuartas-Uribe B., Iborra-Clar A., 2007. Reuse of tannery wastewaters by combination of ultrafiltration and reverse osmosis after a conventional physical-chemical treatment. Desalination 204, 219–226.

Meng, F., Chae, S.-R., Drews, A., Kraume, M., Shin, H.-S., Yang, F., 2009. Recent advances in membrane bioreactors (MBRs): membrane fouling and membrane material. Water Res. 43, 1489–512.

Muhammad Aamir Shahzad, Sher Jamal Khan, Muhammad Saboor Siddique, 2019. Draw solution recovery using direct contact membrane distillation (DCMD) from osmotic membrane bioreactor (Os-MBR). J. Water Process Eng. 30, 2180–2185.

Munz, G., De Angelis, D., Gori, R., Mori, G., Casarci, M., Lubello, C., 2009. The role of tannins in conventional and membrane treatment of tannery wastewater. J. Hazard. Mater. 164, 733–739.

Muthu, S., Childress, A., Brant, J., 2014. Propagation-of-uncertainty from contact angle and streaming potential measurements to XDLVO model assessments of membrane-colloid interactions. J. Colloid Interface Sci. 428, 191–198.

Moser P.B., Clara Bretas, Eduardo Coutinho Paula, Clara Faria, Bárbara C. Ricci, Ana Cláudia F.P. Cerqueira, M.C.S.A., 2019. Comparison of hybrid ultrafiltration-osmotic membrane bioreactor and conventional membrane bioreactor for oil refinery effluent treatment.

Qiu, G., Law, Y.M., Subhabrata, D., Ting, Y., 2015. Direct and complete phosphorus recovery from municipal wastewater using a hybrid microfiltration-forward osmosis membrane bioreactor process with seawater brine as draw solution. Environ. Sci. Technol. 49, 6156–6163.

Ryan W. Holloway, Andrea Achilli. and Cath T.Y., 2015. The osmotic membrane bioreactor: a critical review. Environ. Sci. Water Res. Technol. 1, 581–605.

Srinivasa-Raghavan, D.S., Qiu, G., Ting, Y.P., 2018. Fate and removal of selected antibiotics in an osmotic membrane bioreactor. Chem. Eng. J. 334, 198–205.

Susanto, H., Ulbricht, M., 2007. Photografted thin polymer hydrogel layers on PES ultrafiltration membranes: characterization, stability, and influence on separation performance. Langmuir 23, 7818–7830.

Van Huy Tran, Sungil Lim, Dong Suk Han, Nirenkumar Pathak, Nawshad Akther, Sherub Phuntsho, Hyunwoong Park, Ho Kyong Shon, 2019. Efficient fouling control using outer-selective hollow fiber thin-film composite membranes for osmotic membrane bioreactor applications. Technol. Bioresour. 282, 9–17.

Vatanpour, V., Esmaeili, M., Hossein, M., Abadi, D., 2014. Fouling reduction and retention increment of polyethersulfone nano fi ltration membranes embedded by amine-functionalized multi-walled carbon nanotubes. J. Memb. Sci. 466, 70–81.

Wang, X., Chang, V.W.C., Tang, C.Y., 2016. Osmotic membrane bioreactor (OMBR) technology for wastewater treatment and reclamation: Advances, challenges, and prospects for the future. J. Memb. Sci. 504, 113–132.

Wang, X., Chen, Y., Yuan, B., Li, X., Ren, Y., 2014a. Impacts of sludge retention time on sludge characteristics and membrane fouling in a submerged osmotic membrane bioreactor. Bioresour. Technol. 161, 340–7.

Wang, X., Wang, C., Tang, C.Y., Hu, T., Li, X., Ren, Y., 2017. Development of a novel anaerobic membrane bioreactor simultaneously integrating micro fi ltration and forward osmosis membranes for low- strength wastewater treatment. J. Memb. Sci. 527, 1–7.

Wang, X., Yuan, B., Chen, Y., Li, X., Ren, Y., 2014b. Integration of micro-filtration into osmotic membrane bioreactors to prevent salinity build-up. biores 167, 116–123.

Xie, M., Price, W.E., Nghiem, L.D., 2012. Rejection of pharmaceutically active compounds by forward osmosis: Role of solution pH and membrane orientation. Sep. Purif. Technol. 93, 107–114.

Yang, E., Chae, K.J., Alayande, A.B., Kim, K.Y., Kim, I.S., 2016. Concurrent performance improvement and biofouling mitigation in osmotic microbial fuel cells using a silver nanoparticle-polydopamine coated forward osmosis membrane. J. Memb. Sci. 513, 217–225.

Yang, W., Cicek, N., Ilg, J., 2006. State-of-the-art of membrane bioreactors : Worldwide research and commercial applications in North America. J. Memb. Sci. 270, 201–211.

Zhang, B., Song, X., Nghiem, L.D., Li, G., Luo, W., 2017. Osmotic membrane bioreactors for wastewater reuse: Performance comparison between cellulose triacetate and polyamide thin film composite membranes. J. Memb. Sci. 539, 383–391.

Zhang, J., Lay, W., Loong, C., Chou, S., Tang, C., Wang, R., Gordon, A., 2012. Membrane biofouling and scaling in forward osmosis membrane bioreactor. J. Memb. Sci. 404, 8–14.

Zou, S., Wang, Y.-N., Wicaksana, F., Aung, T., Wong, P.C.Y., Fane, A.G., Tang, C.Y., 2013. Direct microscopic observation of forward osmosis membrane fouling by microalgae: Critical flux and the role of operational conditions. J. Memb. Sci. 436, 174–185.

Zuriaga-Agustí, E., Bes-Piá, A., Mendoza-Roca, J.A., Alonso-Molina, J.L., 2013. Influence of extraction methods on proteins and carbohydrates analysis from MBR activated sludge flocs in view of improving EPS determination. Sep. Purif. Technol. 112, 1–10.